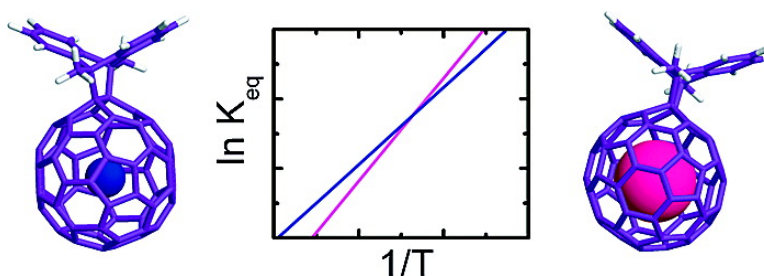


Effect of Xenon on Fullerene Reactions

Michael Frunzi, R. James Cross, and Martin Saunders

J. Am. Chem. Soc., **2007**, 129 (43), 13343-13346 • DOI: 10.1021/ja075568n • Publication Date (Web): 09 October 2007

Downloaded from <http://pubs.acs.org> on February 14, 2009



More About This Article

Additional resources and features associated with this article are available within the HTML version:

- Supporting Information
- Access to high resolution figures
- Links to articles and content related to this article
- Copyright permission to reproduce figures and/or text from this article

[View the Full Text HTML](#)

Effect of Xenon on Fullerene Reactions

Michael Frunzi, R. James Cross,* and Martin Saunders*

Contribution from the Department of Chemistry, Yale University, P.O. Box 208107, New Haven, Connecticut 06520

Received July 25, 2007; E-mail: james.cross@yale.edu; ms@gaus90.chem.yale.edu

Abstract: Solutions containing ${}^3\text{He}@C_{60}$, ${}^{129}\text{Xe}@C_{60}$, and varying amounts of 9,10-dimethylantracene (DMA) were allowed to reach equilibrium, and the ${}^3\text{He}$ and ${}^{129}\text{Xe}$ NMR spectra were taken at the same temperature. Each spectrum showed peaks for the unreacted $X@C_{60}$ and for the monoadduct. The ratios of the peak heights show that the included xenon atom substantially changes the equilibrium constant. This change is temperature dependent, meaning that the xenon atom changes both ΔH and ΔS for the reaction. DMA is more reactive with $\text{He}@C_{60}$ at low temperatures and with $\text{Xe}@C_{60}$ at higher temperatures. The difference in chemical shift between the monoadduct and the unreacted $X@C_{60}$ is more than twice as large for Xe than for He and in the opposite direction. Calculations show that the electron density in $\text{Xe}@C_{60}$ is higher than that in empty C_{60} on the outside of the cage.

Introduction

When two atoms or groups approach one another, the interaction energy can be large (two H atoms forming H_2) or very small (two He atoms at the minimum of the van der Waals curve). A considerable amount of chemistry is devoted to empirically measuring and theoretically understanding non-bonding interactions. Because of their unreactive nature, noble gas atoms are important in studying these interactions. There is a large difference between helium, which can be treated as a hard sphere in most cases, and xenon, which is large and polarizable and displays a strong van der Waals attraction with almost everything. By placing these atoms inside C_{60} and other fullerenes, we have made systems where the noble gas interacts with the same fullerene surface. Interaction energies for helium are expected to be small, but for krypton and xenon, they are larger and attractive.

We have long used ${}^3\text{He}$ NMR spectroscopy to study reactions of fullerenes.^{1–3} ${}^3\text{He}@C_{60}$ can be made by heating C_{60} in the presence of ${}^3\text{He}$ at high pressures.^{4,5} Because the electrons on C_{60} affect the magnetic field inside the cage, the NMR resonance for ${}^3\text{He}@C_{60}$ is shifted upfield by 6.3 ppm from the resonance in ${}^3\text{He}$ dissolved in solution. Chemical reactions on the C_{60} cage alter the magnetic field inside and change the position of the resonance. As an example, Hirsch et al. showed that 9,10-dimethylantracene (DMA) adds reversibly via a Diels–Alder

reaction to C_{60} at room temperature.⁶ By varying the concentration of DMA, we found one monoadduct, six bis adducts, 11 tris adducts, and 10 tetrakis adducts, each giving a unique line in the ${}^3\text{He}$ NMR.⁷ Measuring the ratios of peak areas gave all the equilibrium constants. By repeating the experiment at various temperatures, we obtained ΔH and ΔS for the reaction. Because helium is small, and its electrons are tightly bound, the presence of ${}^3\text{He}$ probably does not affect the equilibrium. What about heavier noble gases? The only other spin-1/2 noble gas is ${}^{129}\text{Xe}$, and we have made ${}^{129}\text{Xe}@C_{60}$ and measured the ${}^{129}\text{Xe}$ NMR spectrum.⁸ The 5p electrons on xenon should interact strongly with the π electrons on C_{60} . This interaction could change the equilibrium constants and might mean that the ${}^{129}\text{Xe}$ NMR spectroscopy would be quite different than the ${}^3\text{He}$ NMR spectroscopy. Here, we measure the effect of an included xenon atom on both the position of the NMR resonances and on the equilibrium constants for DMA addition



In this study, an amount of ${}^{129}\text{Xe}@C_{60}$ was combined with ${}^3\text{He}@C_{60}$ in the same sample, and DMA was added. The same concentration of free DMA was available for equilibrium with each endohedral species. Using both ${}^3\text{He}$ and ${}^{129}\text{Xe}$ NMR, we can obtain the ratio of the equilibrium constant for ${}^3\text{He}@C_{60}$ to that for ${}^{129}\text{Xe}@C_{60}$. We do not have to measure the concentration of free DMA since it is the same for both equilibria.

Experimental Procedures

Labeling of C_{60} . Both ${}^3\text{He}@C_{60}$ and ${}^{129}\text{Xe}@C_{60}$ were prepared according to the high-pressure method developed by Khong et al.⁵ C_{60} and KCN were ground in a ball mill into a fine powder. This mixture

- (1) Saunders, M.; Jiménez-Vázquez, H. A.; Bangerter, B. W.; Cross, R. J.; Mroczkowski, S.; Freedberg, D. I.; Anet, F. A. L. *J. Am. Chem. Soc.* **1994**, *116*, 3621–3622.
- (2) Saunders, M.; Cross, R. J.; Jiménez-Vázquez, H. A.; Shimshi, R.; Khong, A. *Science* **1996**, *271*, 1693–1697.
- (3) Saunders, M.; Cross, R. J. Putting Nonmetals into Fullerenes. In *Endofullerenes: A New Family of Carbon Clusters*; Akasaka, T., Nagase, S., Eds.; Kluwer: Dordrecht, The Netherlands, 2002; Vol. 3, pp 1–11.
- (4) Saunders, M.; Jiménez-Vázquez, H. A.; Cross, R. J.; Mroczkowski, S.; Gross, M. L.; Giblin, D. E.; Poreda, R. J. *J. Am. Chem. Soc.* **1994**, *116*, 2193–2194.
- (5) Cross, R. J.; Khong, A.; Saunders, M. *J. Org. Chem.* **2003**, *68*, 8281–8283.

- (6) Lamparth, I.; Herzog, A.; Hirsch, A. *Tetrahedron* **1996**, *52*, 5065–5075.
- (7) Wang, G. W.; Saunders, M.; Cross, R. J. *J. Am. Chem. Soc.* **2001**, *123*, 256–259.
- (8) Syamala, M. S.; Cross, R. J.; Saunders, M. *J. Am. Chem. Soc.* **2002**, *124*, 6216–6219.

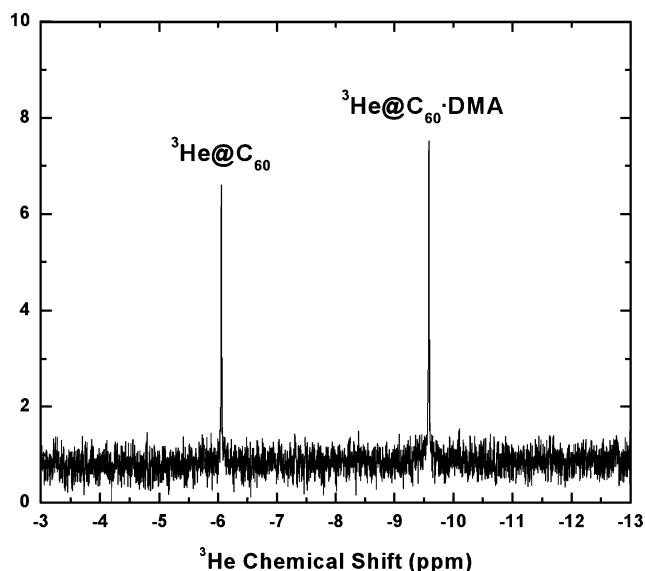


Figure 1. ^3He NMR spectrum showing unreacted C_{60} and monoadduct. Shifts are relative to dissolved ^3He gas.

was put into a copper tube and, while being cooled with liquid nitrogen, 1 atm of helium or xenon gas was added. In both cases, isotopically enriched gas from Spectra Gases was used (99.9 and 86 atom %, respectively). The tubes were placed in a high-pressure vessel and heated at 650 °C at 3000 atm for 8 h. Afterward, the product was dissolved in CS_2 and filtered. Typical yields for this procedure were 30 mg of C_{60} containing $\sim 1\%$ $^3\text{He}@C_{60}$ or $\sim 0.3\%$ $^{129}\text{Xe}@C_{60}$.

HPLC Procedure. $\text{Xe}@C_{60}$ was separated from C_{60} to increase the ^{129}Xe NMR signal, using a procedure described by Syamala et al.⁸ A total of 300 mg of unseparated $^{129}\text{Xe}@C_{60}$ was initially dissolved in *o*-dichlorobenzene, yielding a concentration of ~ 6 mg/mL. This was injected onto a PYE column in 100 μL volumes and eluted with toluene at a rate of 2.0 mL/min. The latter part of the C_{60} peak was reinjected several times, each time discarding the empty fraction. After the third pass, a small peak representing $\text{Xe}@C_{60}$ became visible. The final sample contained approximately 30% $^{129}\text{Xe}@C_{60}$.

Sample Preparation. The NMR sample contained ~ 1 mg of $^{129}\text{Xe}@C_{60}$ and 5 mg of $^3\text{He}@C_{60}$ dissolved in 750 μL of *o*-dichlorobenzene. Next, 250 μL of C_6D_6 was added for the deuterium lock and 5 mg of $\text{Cr}(\text{acac})_3$ as a relaxation agent. Initially, ~ 0.25 equiv of DMA was added, and the tube was pumped down to vacuum and sealed to prevent the oxidation of C_{60} and DMA as well as solvent evaporation. The 0.2 M DMA stock solution added a negligible volume to the sample so as not to disturb the concentration dependent equilibrium measurement. Further amounts of DMA were added in later experiments.

^3He NMR Spectroscopy. The NMR spectrum was taken on a Bruker Avance 500 MHz spectrometer running at a ^3He frequency of 380.9 MHz. Typically, 800 pulses were used with a width of 7 μs and a recycling delay of 2 s. All chemical shifts were relative to the known resonance of ^3He dissolved in solution. Line broadening of up to 1 Hz was used to improve the signal-to-noise ratio. Figure 1 shows a ^3He spectrum for the reaction mixture after 1.0 molar equiv of DMA was added.

^{129}Xe NMR Spectroscopy. The ^{129}Xe NMR spectrum was taken on a different Bruker Avance 500 MHz spectrometer running at a ^{129}Xe frequency of 138.3 MHz. Typically, 12 000 pulses were required with a width of 6.2 μs and a recycling delay of 3 s. All chemical shifts were relative to the known resonance of ^{129}Xe dissolved in solution. Line broadening of 1.6 Hz was used to improve the signal-to-noise ratio. Figure 2 shows a ^{129}Xe spectrum for the reaction mixture after 1.0 molar equiv of DMA was added.

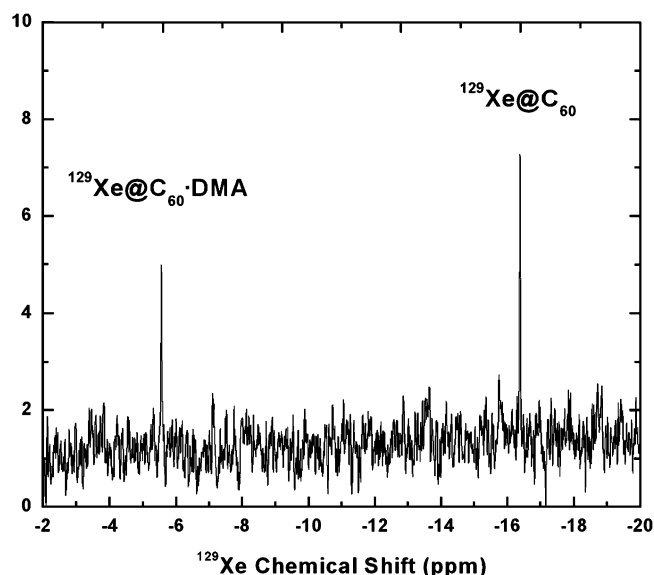


Figure 2. ^{129}Xe NMR spectrum showing unreacted C_{60} and monoadduct. Shifts are relative to dissolved ^{129}Xe gas.

Table 1. Chemical Shifts of Noble Gas Atoms Inside C_{60} and $\text{C}_{60}\cdot\text{DMA}$ Relative to Noble Gas Dissolved in Same Solvent at 25 °C

guest atom (X)	$\text{X}@C_{60}$ δ (ppm) ^a	$\text{X}@C_{60}\cdot\text{DMA}$ δ (ppm) ^a	difference δ (ppm)
^3He	-6.04	-9.57	-3.53
^{129}Xe	-16.4	-5.6	+10.8

^a Relative to free ^3He or ^{129}Xe dissolved in the solvent.

Results and Discussion

The spectra in Figures 1 and 2 show two very clear, distinct differences. The difference in the chemical shift for $^{129}\text{Xe}@C_{60}\cdot\text{DMA}$ and $^{129}\text{Xe}@C_{60}$ is both larger and of the opposite sign than in the helium case. Table 1 lists the chemical shifts.

Previous studies found that the $^{129}\text{Xe}@C_{60}$ resonance shifted by about -8.9 ppm from the resonance for dissolved ^{129}Xe , instead of -16.4 shown here. However, the previous work was conducted in $\text{C}_6\text{H}_6/\text{C}_6\text{D}_6$, and the frequency of the dissolved ^{129}Xe gas signal was known to be highly dependent on both solvent and temperature.⁹ Noting the differences in chemical shift, the magnetic field within the reacted fullerene must have very different effects on the guest nuclei. The helium case is more easily explained. The helium atom is small, its electrons are tightly bound, and it interacts only slightly with the fullerene cage. Indeed, the chemical shift can be fairly accurately calculated by using a ghost atom that just samples the magnetic field inside C_{60} .¹⁰ Making the DMA adduct changes the electronic distribution in the cage and thus changes the magnetic field inside. However, the ^{129}Xe case is less straightforward. The 5p electrons on xenon clearly interact with the π electrons on C_{60} , and this causes a change in chemical shift that is due to more than just magnetic shielding by the C_{60} electrons. The formation of the DMA adduct clearly changes this interaction in ways more complicated than in the helium case.

The second striking feature is that at room temperature, K_{eq} for the monoaddition of DMA to $\text{He}@C_{60}$ is twice the K_{eq} for

(9) Miller, K. W.; Reo, N. V.; Uiterkamp, A.; Stengle, D. P.; Stengle, T. R.; Williamson, K. L. *Proc. Natl. Acad. Sci. U.S.A.* **1981**, *78*, 4946–4949.
(10) Bühl, M. *Chem.—Eur. J.* **1998**, *4*, 734–739.

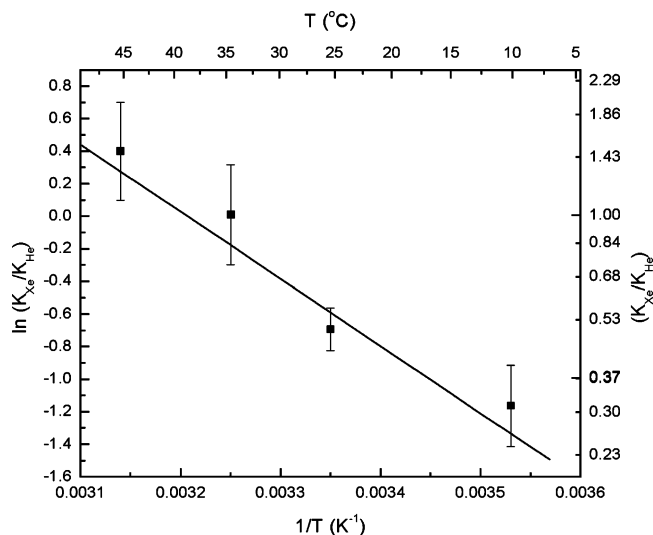


Figure 3. van't Hoff plot of natural logarithm of ratio of equilibrium constants vs $1/T$. Error bars are calculated from the signal-to-noise ratio of the NMR signals (mostly due to ^{129}Xe).

Table 2. Thermodynamic Parameters from the van't Hoff Plot

	$^3\text{He}@C_{60}^a$	change ^b	$^{129}\text{Xe}@C_{60}$
ΔH reaction (kJ/mol)	-95.7	-0.5	-95.2
ΔS reaction (J mol K^{-1})	-255.8	-1.6	-254.2

^a Taken from ref 7. ^b From the van't Hoff plot.

$\text{Xe}@C_{60}$. It is clear that the incorporation of a xenon atom into the C_{60} cage changes the chemistry of the molecule. Let

$$R = K_{\text{eq}}(^{129}\text{Xe})/K_{\text{eq}}(^3\text{He}) \quad (2)$$

for reaction 1. Assuming that ΔH stays constant over the temperature range, the van't Hoff plot of $\ln R$ versus $1/T$ should give a straight line with a slope of $-\Delta\Delta H/R$ and an intercept of $\Delta\Delta S/R$, where $\Delta\Delta H = \Delta H(^{129}\text{Xe}) - \Delta H(^3\text{He})$. Figure 3 shows the van't Hoff plot, and Table 2 gives the results. Previous work showed that reaction 1 is exothermic with a decrease in entropy.⁷ The present work shows that adding xenon to C_{60} increases both ΔH and ΔS , making the reaction less exothermic but with a smaller entropy loss. Thus, the addition to ^3He is favored at low temperatures (lower enthalpy) and to ^{129}Xe at higher temperatures (higher entropy).

We added more DMA to the sample to look for the bis adducts. This was done at 5 °C, where K_{eq} is large. The ^3He NMR spectrum showed no measurable amount of unreacted C_{60} , a small amount of monoadduct, and the three largest peaks previously found for the bis adducts (85% of the bis adduct). The ^{129}Xe NMR spectrum, however, showed some unreacted C_{60} , lots of monoadduct, and a few peaks, just above the noise that might or might not be bis adducts. We conclude that K_{eq} for the equilibrium between the mono- and bis adducts is smaller for ^{129}Xe than for ^3He , as in the case for the formation of the monoadduct.

It is not clear as to why the incorporation of a xenon atom changes the thermodynamics of the addition reaction. We initially thought that perhaps the reaction with the DMA molecule squeezes the C_{60} cage in one direction and that the xenon atom inside would resist the contortion and therefore

inhibit the reaction. Gaussian 03¹¹ structure optimization of C_{60} and $C_{60}(\text{DMA})$ with Hartree–Fock and the DFT MPWB1K functional using the 6-31g(d,p) basis set shows that the 58 carbons not involved in the bonding to DMA move by at most 0.05 Å. Those formed in the bonds to DMA move away from the center by 0.38 Å. These results agree with recent experiments using EPR to probe $\text{N}@C_{60}(\text{DMA})$.¹² Thus, cage distortion cannot account for the effect.

We calculated the incorporation energy of $\text{Xe}@C_{60}$ using various methods in Gaussian 03.¹¹ The calculations were possible due to the high I_h symmetry of the molecule. Calculations involving atoms as large as xenon can be problematic for most basis sets, so in this case, we have used the Wood–Boring quasi-relativistic pseudo-potential.¹³ When calculated with RHF or B3LYP with the 6-31g(d) basis set, the incorporation of xenon into C_{60} is shown to be highly endoergic by 134.7 kJ/mol (32.2 kcal/mol). This result is nonphysical since it predicts that $\text{Xe}@C_{60}$ cannot be formed. Using the MP2 method, $\text{Xe}@C_{60}$ becomes energetically favorable by -165.3 kJ/mol (-39.5 kcal/mol). This seems too large, so we used a counterpoise correction. When a calculation is performed for $\text{Xe}@C_{60}$, the C_{60} moiety can use the basis functions for Xe, and the Xe atom can use the basis functions for C_{60} . Increasing the size of the basis set will cause the total energy to decrease, regardless of any interaction between the xenon and the C_{60} . The correction first finds the energy of the molecule with the xenon atom replaced with a ghost atom surrounded by empty orbitals and then does the same with ghost atoms in place of carbon atoms. These energies are subtracted and applied as a correction. The counterpoise correction changes the incorporation energy to -54 kJ/mol (-12.9 kcal/mol). This differs from Bühl's calculated energy of -22.6 kJ/mol (-5.4 kcal/mol) also found using the MP2 method but with a different basis set.¹⁴ Clearly, the calculation of the incorporation energy of xenon into C_{60} is highly dependent on both the basis set and the method used, and one can have little confidence in the result. However, the results show quite clearly that xenon interacts strongly with C_{60} . Single-point MP2 calculations on structures optimized at RHF/6-31g-(d,p) show that going from $\text{Xe}@C_{60}$ to $\text{Xe}@C_{60}\cdot\text{DMA}$ is energetically less favorable than for C_{60} going to $C_{60}\cdot\text{DMA}$ by a mere 3 kJ/mol. The loss of symmetry prevents us from using more accurate methods. Given the previous discussion, this result is likely meaningless.

Clearly, the presence of the xenon atom changes the electron distribution in C_{60} . In most molecules, one could look at the change in the electric dipole or quadrupole moment, but in C_{60} , the symmetry is high enough that both moments are identically zero. How does one measure what is essentially radial motion in an almost spherical molecule? Using Gaussian 03 and Molekel, we were able to calculate surfaces of constant electron density $S(\rho)$, where ρ is the electron density (electrons/Å³). Except for small values of ρ , the surfaces are lumpy spheres that gradually become larger as ρ decreases. Molekel can then calculate the volume enclosed by the surface, $V(\rho)$. If the xenon atom pushes electrons outward in C_{60} , then, for a given value

- (11) Frisch, M. J.; et al. *Gaussian 03*; Gaussian, Inc.: Pittsburgh, PA, 2003.
- (12) Franco, L.; Ceola, S.; Corvaja, C.; Bolzonella, S.; Harneit, W.; Maggini, M. *Chem. Phys. Lett.* **2006**, *422*, 100–105.
- (13) Nicklass, A.; Dolg, M.; Stoll, H.; Preuss, H. *J. Chem. Phys.* **1995**, *102*, 8942–8952.
- (14) Bühl, M.; Patchkovskii, S.; Thiel, W. *Chem. Phys. Lett.* **1997**, *275*, 14–18.

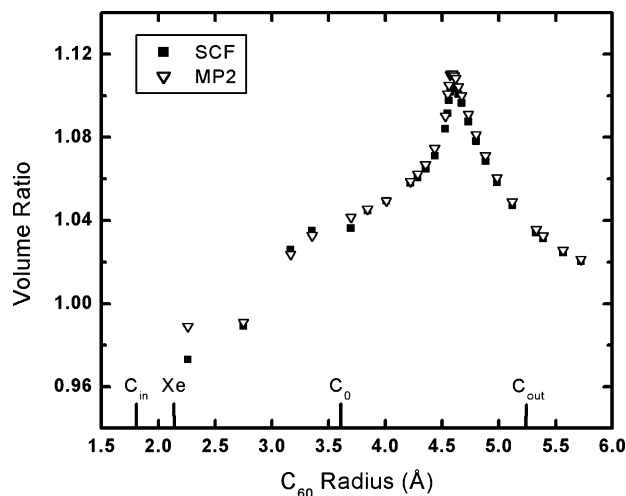


Figure 4. Ratio of volume enclosed by surface of constant electron density in Xe@C₆₀ to the volume for C₆₀ vs radius of C₆₀ (see text), using SCF and MP2 densities.

of ρ , $V(\rho)$ will be larger for Xe@C₆₀ than for C₆₀. Thus, the ratio of volumes is a measure of how the electrons are moved radially. Since the surface is roughly spherical, we can define a radius, $r(\rho)$, such that $V(\rho) = 4\pi r(\rho)^3/3$. In Figure 4, we plot the ratio of $V(\rho)$ for Xe@C₆₀ to $V(\rho)$ for C₆₀ as a function of $r(\rho)$ for C₆₀. As a reference, we also show the radius of the C₆₀ cage (C_0), the van der Waals radius of carbon (C_{in} and C_{out}), and the van der Waals radius of xenon (Xe). A simple reliance on van der Waals radii would predict that Xe@C₆₀ does not exist. It is clear that the xenon atom increases electron density on the outside of the cage. At the maximum (4.6 Å), the electron density in Xe@C₆₀ is 35% greater than in C₆₀. This distance makes sense given that the reactivity of the cage double bonds has changed. The sharp cusp and detailed structure may be dependent on the basis functions used to describe the system.

There are two obvious explanations for the increase in electron density, which do not hold up under close scrutiny. First is the possibility that the diameter of the carbon cage is larger in Xe@C₆₀, and this would naturally increase the electron density. However, the radius of the cage increases only from 3.552 to 3.553 Å (both MP2 calculations), clearly not enough to explain the effect. Second, the increase in electron density could be due simply to the long-range tail of the electron distribution of the xenon atom. However, the electron density of an isolated xenon atom at 4.6 Å is smaller than that in C₆₀ by more than 4 orders of magnitude. The xenon atom appears to be pushing the fullerene electrons outward.

Conclusion

The reactivity of ¹²⁹Xe@C₆₀ was compared to ³He@C₆₀ for the Diels–Alder addition of DMA using ¹²⁹Xe and ³He NMR. It was found that the inclusion of such a large, electron-rich guest increased ΔH of the monoaddition reaction by 0.5 kJ/mol and increased ΔS by 1.6 J/mol K. It is not clear what causes this effect. The closest analogy to conventional chemistry might be to describe it as an unusual solvent effect. In this case, the solvent is inside the molecule and not outside it. Calculations show that the xenon atom increases the electron density in the region just outside the carbon cage. Also, chemical shift of the ¹²⁹Xe nucleus within the monoadduct is much larger and has a different sign than the corresponding helium-containing material.

Acknowledgment. Research support from the National Science Foundation under Grant CHE-0307168 is gratefully acknowledged. We are grateful to Dr. Eric Paulson for help in taking and interpreting the NMR data.

Supporting Information Available: Complete ref 11. This material is available free of charge via the Internet at <http://pubs.acs.org>.

JA075568N